ChemComm

RSC Publishing

COMMUNICATION

View Article Online
View Journal | View Issue

Cite this: *Chem. Commun.*, 2013, **49**, 4761

Received 6th March 2013,
Accepted 3rd April 2013

DOI: 10.1039/c3cc41708e

www.rsc.org/chemcomm

A squaric acid-stimulated electrocatalytic reaction for sensing biomolecules with cycling signal amplification†

Wenqiang Lai, Dianping Tang,* Libing Fu, Xiaohua Que, Junyang Zhuang and Guonan Chen*

Squaric acid, a 2-dimensional planar structure of squarate C_4O_4 units linked by protons in a layered sheet, was utilized for the first time as a catalytic substrate for ultrasensitive electronic determination of low-abundance proteins by coupling a target-induced electrocatalytic reaction with the *in situ* cycling signal amplification strategy.

Squaric acid (SQA), one of the most studied hydrogen-bonded antiferroelectrics in the KH_2PO_4 family, is a diacid that exhibits two acidic hydroxyl groups with pK_a values of 0.54 and 3.48 as well as two highly polarized carbonyl groups.[1] The high acidity with high pK_a = 0.54 for the first proton and pK_a = 3.48 for the second is attributable to resonance stabilization of the anion. At room temperature, SQA has a 2-dimensional planar structure of squarate C_2O_2 units linked by protons in a layered sheet. Upon the dielectric phase transition, the crystal structure changes from the monoclinic (AFE phase; $P2_1/m$, $Z = 2$) to the tetragonal form (PE phase, $I4/m$, $Z = 1$).[2] More inspiringly, the four-membered ring of SQA remains intact with oxidizing agents under mild conditions, and produces cyclobutaneoctol as the product, the tetrahydrate of cyclobutanetetrone.[3] Upon reduction with reducing agents, the produced cyclobutaneoctol is converted into SQA.

The unique structure provides not only versatile proton acceptor sites at the carbonyl function for hydrogen bonding but also binding sites to metal ions.[4] With univalent metals, *e.g.* potassium, squaric acid forms salts which are readily soluble in water, whereas the squarates of bivalent and tervalent metals are insoluble.[5] Another, quantum mechanical, way of describing the dianion is to assume that π electrons of the two double-bonded oxygen atoms are shifted to the latter, so that all four oxygens become single-bonded $-O^-$ groups and a double positive electric charge is left in the ring of carbon atoms.

Nowadays, squaric acid is mainly applied for the synthesis of its derivatives and in immunotherapy.[6] To the best of our knowledge, however, there is no report focusing on squaric acid in electroanalytical chemistry. The reason might be attributed to the weak redox properties of SQA or the unaffordable conjugation with biomolecules. Significantly, Das *et al.* found that C–OH in the *p*-aminophenol could be initially electrochemically oxidized to C═O through the ferrocene mediator, and then reduced back to C–OH by $NaBH_4$.[7] The catalytic recycling process between C–OH and C═O caused the amplification of the electrochemical signal. Unfortunately, the amount of the hydroxyl groups in the *p*-aminophenol molecule was limited. To improve this, Akanda *et al.* constructed another redox cycling protocol by using L-ascorbic acid with two available hydroxyl groups.[8] The signal was amplified through two –OH groups based on the redox cycling between L-ascorbic acid and dehydroascorbic acid. In this regard, our motive was to utilize SQA with two C–OH and two C═O groups as the catalytic substrate for the amplification of electrocatalytic signal through the cycling between squaric acid, cyclobutaneoctol and cyclobutanetetrone.

Herein, we report a novel and enzyme-free electrochemical immunoassay for sensing a low-abundance protein (alpha-fetoprotein, AFP, used as a model) by coupling with the SQA-stimulated redox recycling strategy. The assay was carried out in pH 7.4 PBS containing 1.0 mM squaric acid and 1.0 mM tris(2-carboxyethyl)phosphine (TCEP, as a reducing agent, which can reduce electroactive organic materials such as dehydroascorbic acid and quinone at a fast rate) by using ferrocenecarboxylic acid-labelled *anti*-AFP polyclonal antibody (Fc-pAb_2) as trace tags with a sandwich-type immunoassay mode (Scheme 1). Mouse monoclonal *anti*-AFP capture antibody (mAb_1) was directly immobilized on the surface of glassy carbon electrode (GCE) *via* the electrochemically deposited nanogold–graphene hybrid nanostructures (AuNP–GP). In the presence of the target analyte, the immobilized mAb_1 and Fc-pAb_2 sandwich the target AFP. During the electrochemical measurement, the added squaric acid (SQA) was reduced to cyclobutaneoctol (CBO) by TCEP, then the generated CBO was oxidized step by step to cyclobutanetetrone (CBT) by the labelled ferrocene on the Fc-pAb_2, and then the resulting CBT was reduced again back to CBO by TCEP. The self-produced CBO reactant was catalytically recycled between the CBO and CBT, thereby resulting in the amplification of the electrochemical signal (please see experimental details in the ESI†). Under the fixed SQA and TCEP, the signal directly depends on the labelled ferrocene relative to the target AFP level.

In this work, mAb_1 was immobilized onto the sensor through the strong interaction between AuNP–GP and mAb_1. To verify the

Ministry of Education & Fujian Provincial Key Laboratory of Analysis and Detection of Food Safety, Department of Chemistry, Fuzhou University, Fuzhou 350108, P.R. China. E-mail: dianping.tang@fzu.edu.cn; Fax: +86 591 22866135; Tel: +86 591 22866125

† Electronic supplementary information (ESI) available: Experimental procedures and characterization. See DOI: 10.1039/c3cc41708e

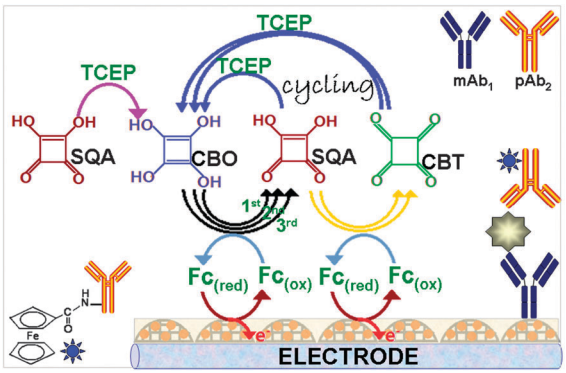

Scheme 1 Schematic illustration of the SQA-stimulated electrocatalytic reaction for sensing low-abundance protein based on the cycling signal amplification strategy.

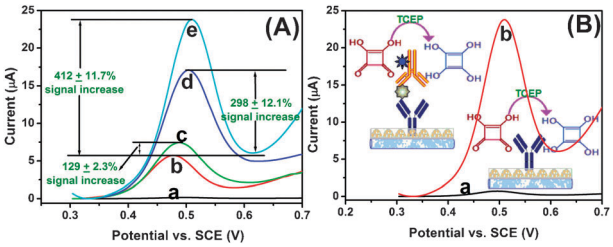

Fig. 2 (A) DPV responses of (a) the newly prepared mAb_1/AuNP–GP/GCE in pH 7.4 PBS, (b) electrode '*a*' after 0.1 ng mL^{-1} AFP and Fc-pAb_2 in pH 7.4 PBS, (c) electrode '*b*' in pH 7.4 PBS + 1.0 mM SQA, (d) electrode '*b*' in pH 7.4 PBS + 1.0 mM CBO, and (e) electrode '*b*' in pH 7.4 PBS + 1.0 mM SQA + 1.0 mM TCEP. (B) DPV responses of (a) the mAb_1/AuNP–GP/GCE, and (b) electrode '*a*' after 0.1 ng mL^{-1} AFP and Fc-pAb_2 in pH 7.4 PBS containing 1.0 mM SQA and 1.0 mM TCEP.

formation of AuNP–GP on the sensor by the electrochemically deposited method, SEM images of variously modified electrodes were investigated. As seen from Fig. 1A and B, nanogold particles and graphene nanosheets could be simultaneously deposited onto the sensor with homogeneous dispersion. Logically, an important question to be answered was whether the electrodeposited graphene nanosheets were the reduced graphene or graphene oxide owing to the weak conductivity of graphene oxide. As seen from curve '*a*' in the inset of Fig. 1B, a strong D peak and a relatively weak G peak could be observed from the Raman spectra of the newly prepared graphene oxide by the Hummers method.[9] In contrast, a weak D peak and a relatively strong G peak appeared at the electrodeposited graphene nanosheets (curve '*b*'), indicating the presence of the reduced graphene.[10] The successful preparation of AuNP–GP could provide a precondition for the development of the immunoassay.

To realize our design, the newly prepared immunosensor was used for the detection of 0.1 ng mL^{-1} AFP (used as an example), and the characteristics were investigated in pH 7.4 PBS by using differential pulse voltammetry (DPV) in the different supporting electrolytes after each step (Fig. 2A). No peak was observed at the immunosensor (curve '*a*'). When the immunosensor was incubated with the target AFP and Fc-pAb_2, however, an obvious peak current was achieved (curve '*b*'), which was mainly derived from the labelled ferrocene on the Fc-pAb_2. Upon the addition of 1.0 mM SQA in PBS, the current increased (curve '*c*' in Fig. 2A, Δi = 1.7 μA *vs.* curve '*b*'). The reason might be due to the fact that the added SQA was oxidized to CBT by the labelled ferrocene. For comparison, CBO was directly used in pH 7.4 PBS. As seen from curve '*d*' in Fig. 2A, the peak current was obviously higher than that of SQA (curve '*c*'), which might be attributed to the fact that the added CBO was oxidized to SQA/CBT by the conjugated ferrocene. More inspiringly, the peak current further increased when 1.0 mM TCEP was injected into the PBS–SQA system (curve '*e*' in Fig. 2A). The added SQA and TCEP could cause 412 ± 11.7% signal increases in the current (*vs.* curve '*b*'), which was higher than those of SQA and CBO alone. As the control test, the as-prepared immunosensor was monitored before and after incubation with 0.1 ng mL^{-1} AFP and Fc-pAb_2 in pH 7.4 PBS containing 1.0 mM SQA and 1.0 mM TCEP (Fig. 1B). As indicated from curve '*a*', almost no peak current was acquired at the immunosensor. In contrast, a strong peak current was obtained after the formation of the sandwiched immunocomplex on the immunosensor (curve '*b*'). These results indicated that (i) the non-specific adsorption of the immunosensor was negligible, (ii) the peak current mainly derived from the interaction of the labelled ferrocene with the SQA/TCEP, and (iii) the detectable signal could be further amplified by TCEP. Hence, SQA could be preliminarily utilized for the detection of target AFP with the help of TCEP by the designed routine.

To further clarify the *in situ* amplified efficiency by using SQA in the developed immunoassay, L-ascorbic acid, as a similar catalytic substrate to SQA, was also employed as a substitute of the SQA for the determination of AFP standards with various concentrations on immunosensors of the same batch. The obtained results were compared with those of the SQA-based immunoassay system. As seen from Fig. 3, the electrochemical immunoassay by using SQA as a catalytic substrate could exhibit higher current responses than that using L-ascorbic acid. Meanwhile, we also found that use of SQA could enhance the sensitivity (*i.e.* the slope) of the electrochemical immunoassay. The reason might most likely be a consequence of the fact that L-ascorbic acid has only two available –OH groups for the development of the catalytic recycling, whereas SQA has four available groups. Within the same scanning time, the SQA could transfer more electrons than L-ascorbic acid, thus resulting in the strong electrochemical signal and high sensitivity.

Using Fc-pAb_2 as trace tags, the sensitivity and dynamic range of the electrochemical immunoassay were investigated toward AFP standards in pH 7.4 PBS containing 1.0 mM SQA and 1.0 mM TCEP. As seen from the inset in Fig. 4a, DPV peak currents increased with the increasing AFP concentrations. A linear dependence between the peak currents and the logarithm of AFP was obtained in the range from 1.0 pg mL^{-1} to 200 ng mL^{-1} with a detection limit (LOD) of 0.6 pg mL^{-1} estimated at a signal-to-noise ratio of 3 (n = 18) (Fig. 4a). The LOD was partially lower than those of other AFP detection method strategies (Table S1, ESI†). Since the threshold of AFP in normal humans is about 10 ng mL^{-1}, the electrochemical immunoassay can completely

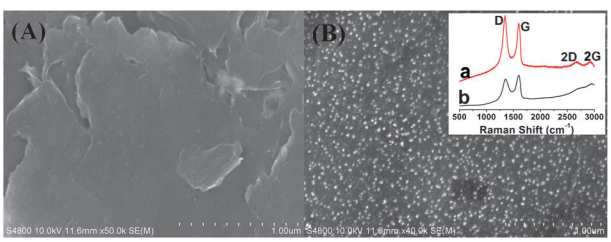

Fig. 1 SEM images of (A) the electrodeposited graphene nanosheets and (B) AuNP–GP nanostructures (inset: typical Raman spectra of (a) graphene oxide and (b) the electrodeposited graphene nanosheets).

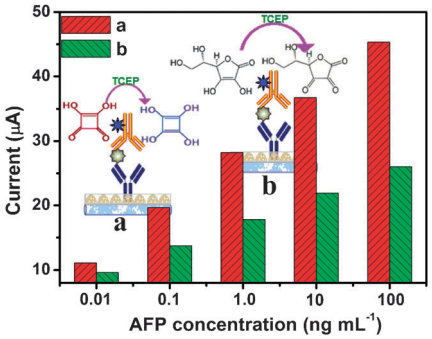

Fig. 3 Comparison of electrochemical responses of the as-prepared immunosensor toward AFP standards with various concentrations using different catalytic substrates in pH 7.4 PBS containing (a) 1.0 mM SQA and 1.0 mM TCEP, (b) 1.0 mM L-ascorbic acid and 1.0 mM TCEP.

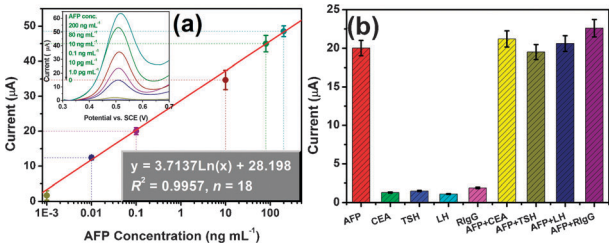

Fig. 4 (a) Calibration plots of the electrochemical immunoassay toward AFP standards in pH 7.4 PBS containing 1.0 mM SQA and 1.0 mM TCEP (inset: the corresponding DPV curves). (b) The specificity of the electrochemical immunoassay (0.1 ng mL^{-1} AFP and 100 ng mL^{-1} interfering agents used in this case).

meet the requirement of clinical diagnostics. Although the system has not yet been optimized for maximum efficiency, importantly, the sensitivity of using SQA as the enhancer was over 1000-fold lower than that of commercially available AFP ELISA kits (1.0 ng mL^{-1}, Genway Biotech. Inc.).[11]

To evaluate the specificity of the developed immunoassay for AFP detection, we challenged the system with other interfering substances, *e.g.* carcinoma embryonic antigen (CEA), thyroid-stimulating hormone (TSH), luteinizing hormone (LH), rabbit IgG (RIgG), uric acid, ascorbic acid, acetaminophen, cholesterol, creatinine, paracetamol, bilirubin, ibuprofen, dopamine, salicylate, tolazamide and tolbutamide. The assay was carried out with the same experimental procedures. As indicated in Fig. 4b and Fig. S4 (ESI†), a significantly higher current was observed with the target AFP than with other proteins. These results indicated that the components coexisting in the sample matrix did not interfere in the determination of AFP, *i.e.*, the electrochemical immunoassay was shown to be sufficiently selective for detection of AFP.

Next, the precision of the developed immunoassay was monitored by assaying 0.01, 1.0 and 100 ng mL^{-1} AFP as examples, using identical batches of immunosensor and Fc-pAb$_2$. Experimental results indicated that the coefficients of variation (CVs, n = 3) of the intra-assay were 7.8, 5.8 and 6.9% for 0.01, 1.0 and 100 ng mL^{-1} AFP, respectively, whereas the CVs of the inter-assay with various batches were 8.9, 6.8 and 8.3% toward the above-mentioned concentrations, respectively. Hence, both intra-assay and inter-assay verified acceptable reproducibility. In addition, the immunosensor displayed satisfactory stability. As much as 90% of the initial current was preserved after storage of the immunosensor and Fc-pAb$_2$ at 4 °C for 30 days.

Finally, the accuracy of the electrochemical immunoassay method was evaluated for testing 10 clinical serum specimens, which were collected from Fujian Provincial Hospital of China according to the rules of the local ethical committee. The obtained results were compared with those of the commercialized electrochemiluminescent immunoassay (ECLIA) method. As shown in Table S2 (ESI†), no significant differences were encountered between the two methods at the 0.05 significance level because all the t_{exp} values in the case were less than t_{crit} ($t_{crit[4,0.05]}$ = 2.77). Hence, the SQA-stimulated electrocatalytic reaction could be regarded as an optional scheme for detecting AFP in real samples.

In summary, this work demonstrates a novel and enzyme-free amplified immunoassay strategy for sensitive electronic detection of low-abundance protein, using an SQA-stimulated electrocatalytic reaction and the cycling signal amplification protocol. Compared with conventional amplified strategies based on enzyme labels or nanolabels, the method is simple, low-cost and highly efficient. Further, SQA with a unique crystal structure can be utilized for the *in situ* amplification of the electrochemical signal. Although the present assay system focuses on the determination of target AFP, it can be easily extended for sensing other biomolecules.

Support from the ''973'' National Basic Research Program of China (2010CB732403), NSFC of China (21075019, 41176079), the Research Fund for the Doctoral Program of Higher Education of China (20103514120003), the China–Russia Bilateral Scientific Cooperation Research Program (21211120157), and the National Science Foundation of Fujian Province (2011J06003) is gratefully acknowledged.

Notes and references

1 (*a*) D. Basak, C. Versek, D. Toscano, S. Christensen, M. Tuominen and D. Venkataraman, *Chem. Commun.*, 2012, **48**, 5922; (*b*) L. Swartz and L. Howard, *J. Phys. Chem.*, 1971, **75**, 1798.
2 (*a*) D. Semmingse, F. Hollander and T. Koetzle, *J. Chem. Phys.*, 1977, **66**, 4405; (*b*) Z. Dega-Szafran, A. Katrusiak and M. Szafran, *J. Mol. Struct.*, 2012, **1030**, 184.
3 (*a*) A. Roedig and G. Markl, *Justus Liebigs Ann. Chem.*, 1960, **636**, 1; (*b*) Y. Huang, Y. Lai and S. Wang, *Chem.–Eur. J.*, 2012, **18**, 8614.
4 (*a*) H. Terao, T. Sugawara, Y. Kita, E. Kaho and S. Takeda, *J. Am. Chem. Soc.*, 2001, **123**, 10468; (*b*) R. West and H. Niu, *J. Am. Chem. Soc.*, 1963, **85**, 2589.
5 (*a*) G. Maahs and P. Hegenberg, *Angew. Chem., Int. Ed. Engl.*, 1966, **5**, 888; (*b*) K. Lee, J. Kweon, I. Oh and C. Lee, *J. Phys. Chem. Solids*, 2012, **73**, 890.
6 (*a*) D. Basak, C. Versek, D. Toscano, S. Christensen, M. Tuominen and D. Venkataraman, *Chem. Commun.*, 2012, **48**, 5922; (*b*) C. Dingels, F. Wurm, M. Wagner, H. Klok and H. Frey, *Chem.–Eur. J.*, 2012, **18**, 16828.
7 J. Das, M. Aziz and H. Yang, *J. Am. Chem. Soc.*, 2006, **128**, 16022.
8 M. Akanda, M. Aziz, K. Jo, V. Tamilavan, M. Hyun, S. Kim and H. Yang, *Anal. Chem.*, 2011, **83**, 3926.
9 W. Hummers and R. Offeman, *J. Am. Chem. Soc.*, 1958, **80**, 1339.
10 Y. Guo, B. Wu, H. Liu, Y. Ma, Y. Yang, J. Zheng, G. Yu and Y. Liu, *Adv. Mater.*, 2011, **23**, 4626.
11 www.genwaybio.com/media/custom/upload/File-1313516446.pdf.